Received 15 December 2023; revised 6 January 2024; accepted 21 January 2024. Date of publication 24 January 2024; date of current version 8 February 2024.

Digital Object Identifier 10.1109/OJCOMS.2024.3358054

A Flexible Polar Decoding Architecture With Adjustable Latency and Reliability

SHINTARO FUJIWARA (Student Member, IEEE), AND HIDEKI OCHIAI (Fellow, IEEE)

Department of Electrical and Computer Engineering, Yokohama National University, Yokohama 240-8501, Kanagawa, Japan

CORRESPONDING AUTHOR: H. OCHIAI (e-mail: hideki@ynu.ac.jp)

This work was supported in part by the Japan Society for the Promotion of Science (JSPS) through the Grants-in-Aid for Scientific Research (KAKENHI) under Grant 21H04873.

ABSTRACT Future mobile and wireless communications should support various applications with their own reliability and latency requirements. Polar codes, adopted in the 5G standard, are capacity achieving as the codeword length increases even with low complexity successive cancellation (SC) decoding. On the other hand, to improve the performance under relatively short codeword lengths, successive cancellation list (SCL) decoding together with the use of cyclic redundancy check (CRC) codes is widely adopted. In this paper, a new design architecture of polar codes is proposed to support applications with diverse reliability and latency requirements. In the proposed approach referred to as a *priority-oriented polar code* (POPC), the information bits are divided into the two parts, *priority bit sequence* (PBS) and *regular bit sequence* (RBS), where the former should be output earlier than the latter in the process of SC or SCL decoding. Theoretical and simulation results show that PBS can be decoded with high reliability and low decoding latency, whereas RBS remains to achieve the same performance as the original decoding approach.

INDEX TERMS Cyclic redundancy check (CRC) codes, polar codes, successive cancellation (SC) decoding, ultra-reliable and low latency communications (URLLC).

I. INTRODUCTION

FUTURE mobile and wireless communications should not only aim at a higher data rate, but also support various reliability and latency requirements imposed by diverse applications, such as those operating under ultra-reliable and low latency communications (URLLC) in the fifth generation (5G) [1]. Considering a use case of 5G, it is also anticipated that network services should simultaneously support various application scenarios using a single physical network [2]. Furthermore, the use case of networks that support *mixed delay traffic* has been envisioned, where those with different latency requirements, such as URLLC and enhanced mobile broadband (eMBB), can coexist [3]. This coexistence is anticipated to allow prospective use cases such as smart manufacturing and unmanned aerial vehicles (UAVs) [4], [5]. In these use cases, two types of data are used for communication between the transmitter and receiver; data for device control and data for payload communication. In general, the control data should be delivered with extremely high reliability and low latency based on the principle of URLLC. In the framework of 5G, the coexistence problem of URLLC with eMBB or massive machine-type communication (mMTC) is discussed in [6], where it is pointed out that re-designing of the physical layer should be inevitable to solve this issue. The coexistence between URLLC and eMBB in multi-cell massive multi-input multi-output (MIMO) system is analyzed further in [7].

Polar codes, adopted in the 5G standard, are the first class of linear error-correcting codes that can achieve Shannon capacity over binary input discrete memoryless symmetric channels with low encoding and decoding complexity based on successive cancellation (SC) decoding [8]. SC decoding requires time and space complexity with only the order of $\mathcal{O}(N \log N)$ for a given codeword length of N. However, the decoding performance of polar codes with moderate codeword length is inferior to those of other capacity approaching codes such as low-density parity-check (LDPC) codes and turbo codes. Subsequently, successive cancellation list (SCL) decoding has been introduced [9], which retains the L most reliable candidates of the estimated input bit sequences at

each stage of SC decoding. In addition, with the help of cyclic redundancy check (CRC) codes as an outer code to select only valid candidates, known as CRC-aided SCL (CA-SCL) decoding, the performance can be significantly improved, making it superior to those of LDPC and turbo codes with moderate codeword length [9]. The price for this improvement is the increasing decoding complexity given by $\mathcal{O}(LN \log N)$. Overcoming this fundamental trade-off between decoding performance and complexity is a challenging problem. To address this issue, a number of approaches have been proposed and examined, such as simplified SC decoding [10], adaptive SCL decoding [11], semi-parallel decoding [12], and simplified list decoding [13], to list a few.

In the conventional CA-SCL decoding, the entire information sequence is protected by CRC code before polar encoding, and the corresponding parity bits are placed at the end of the information sequence. Several other variations have been proposed subsequently, where the information bits are divided into several parts, called *segments*, and each segment is protected by a CRC code of different generator polynomial [14], [15]. More specifically, the partitioned SCL (PSCL) algorithm is introduced in [14], where its main objective is to mitigate memory consumption of SCL decoding. On the other hand, the segmented CA-SCL (SCA-SCL) decoding scheme [15] divides the information bits into several segments of equal length before polar encoding. By decoding each segment successively, the decoding process will be terminated if there is no surviving path that is validated by the corresponding CRC test. Alternatively, the parity bits of a single CRC encoder can be divided into several segments as discussed in [16], [17], [18], [19].

In addition to the above mentioned SC-based decoding, the belief propagation (BP) decoding [20] as well as its extended versions [21], [22] have received significant recent attention due to their capability of performing iterative decoding as well as generating soft-out values.

In this paper, we attempt to design a polar coded system which deals with multiple information sources that have different reliability and latency requirements.[1] More specifically, we consider the two information sequences called *priority bit sequence* (PBS) and *regular bit sequence* (RBS), where the former requires additional reliability with reduced latency compared to the latter, and we then propose a new polar code design architecture which we refer to as a *priority-oriented polar code* (POPC). To this end, we focus on the conventional SC-based decoding schemes, rather than BP-based decoding, as we take advantage of the successive decoding structure of information bits that enables the system to support various latency requirements.

The objective of this paper is to propose a design architecture on PBS and RBS such that they achieve their respective target decoding performance in terms of block error rate (BLER) for a given reference channel signal-to-noise power ratio (SNR). Furthermore, it aims to provide a trade-off among decoding latency, reliability, and information rate (i.e., spectral efficiency) under the framework of SC, SCL, and CA-SCL decoding. For this purpose, we demonstrate through analysis and simulations that polar codes can naturally offer an unequal error protection (UEP) property, where PBS can be decoded with higher reliability and lower decoding latency compared to the original system with SC, SCL, and CA-SCL decoding.

Our low latency decoding architecture has some similarity with the concept of *early termination* or *early stopping* in polar decoding processes. In BP-based decoding, iterative decoding is performed and thus early termination may help reducing the *average* latency as well as power consumption. Therefore, various techniques have been developed (e.g., [23], [24], [25], [26]). For SCL and related decoding, the issue of early termination is discussed in [16], [17], [18], [19], [27], [28], where their main objectives are reduction of memory requirements as well as early detection of erroneous bits in the middle of decoding process, e.g., for smooth retransmission.

The main difference of our architecture from the existing studies is that we aim to output PBS *with guaranteed reliability* in view of URLLC, without sacrificing the decoding reliability of the remaining bits. A similar concept regarding early acquisition of partial data is proposed in [29], where the bit-wise early termination is conducted to reduce the complexity in the iterative multi-user detection process. Since a part of data can be retrieved earlier than the remaining data without degradation of its decoding performance, it may be useful for the tactical surveillance with multiple UAVs that alert to threats, where an instantaneous data acquisition from UAVs plays a critical role [29].

The major contributions of this work are summarized as follows:

- We propose a new polar code design architecture referred to as a *priority-oriented polar code* (POPC), which introduces the concept of PBS and RBS. It is shown that PBS can achieve higher decoding performance than RBS at the same time with lower decoding complexity than the conventional approach.
- We develop design guidelines of PBS length for given decoder models under the condition that it can achieve a target BLER value for a given reference channel SNR over an additive white Gaussian noise (AWGN) channel.
- For SCL decoder, based on an information theoretic analysis, we prove that the reliability of PBS should be enhanced by observing the frozen bits located after PBS, which suggests that the estimated PBS should not be output immediately after the decoder completes processing PBS.

This paper is organized as follows: In Section II, we review the basic notation of polar codes as well as several

[1] In addition to the coexistence between URLLC and eMBB or mMTC [6], other example applications include typical video coding that supports *graceful degradation*; the entire data are divided into low resolution and high resolution classes, where the former class provides an essential image and the latter serves as an enhanced quality.

TABLE 1. A table of abbreviations and notations.

Acronym		Notation	
AWGN	Additive White Gaussian Noise	N	code length
BLER	Block Error Rate	K	entire information length
BP	Belief Propagation	K_{p}, K_{r}	information length of PBS or RBS
BPSK	Binary Phase Shift Keying	K'_{p}	window size of PBS in SCL-based decoder
CA-SCL	CRC-Aided SCL	L	list size of SCL decoder
CRC	Cyclic Redundancy Check	r	length of entire CRC parity bits
LDPC	Low-Density Parity-Check	r_{p}, r_{r}	length of CRC parity bits for PBS or RBS
LLR	Log-Likelihood Ratio	v_1^K	information vector of length K
PBS	Priority Bit Sequence	u_1^N, $\hat{u}_1^N$	input vector of length N and its estimate
POPC	Priority-Oriented Polar Code	x_1^N	codeword vector of length N
RBS	Regular Bit Sequence	y_1^N	received symbol vector of length N
RCA	Reciprocal Channel Approximation	$\mathcal{A}$, $\mathcal{F}$	set of information or frozen bit indices
SC	Successive Cancellation	$\mathbb{F}_2$	binary field
SCA-SCL	Segmented CRC-Aided SCL	$\mathbb{N}$	the set of all natural numbers
SCL	Successive Cancellation List	γ	SNR value
SNR	Signal-to-Noise power Ratio	$P_{\mathrm{BL,p}}$, $P_{\mathrm{BL,r}}$	BLER of PBS or RBS
UAV	Unmanned Aerial Vehicle	$P^*_{\mathrm{BL,p}}$, $P^*_{\mathrm{BL,r}}$	target BLER of PBS or RBS
URLLC	Ultra-Reliable and Low-Latency Communication	$\mathcal{N}(\mu, \sigma^2)$	Gaussian distribution with mean μ and variance σ^2

representative decoding schemes considered throughout this work. In Section III, we describe the proposed polar code design and their decoding approach. In Section IV, we theoretically analyze the performance of PBS decoded by SC and related decoders as well as develop a metric for decoding complexity. The numerical examples based on extensive simulations are presented in Section V. Finally, Section VI concludes this work. The major abbreviations as well as main notations adopted in this paper are provided in Table 1.

II. PRELIMINARY

Throughout this work, following the notation of [8] for vectors of variables, we denote a vector of size N by $x_1^N = (x_1, x_2, \ldots, x_N)$, with its sub-vector given by $x_j^k = (x_j, \ldots, x_k)$ for $1 \le j < k \le N$.

A. POLAR CODES

We consider a symmetric discrete memoryless channel with input alphabet $\mathcal{X} = \{0, 1\}$ and output alphabet $\mathcal{Y}$. With N representing the length of codeword (i.e., blocklength), polar encoding is expressed by $x_1^N = u_1^N G_N$, where $x_1^N = (x_1, \ldots, x_N) \in \mathbb{F}_2^N$, $u_1^N = (u_1, \ldots, u_N) \in \mathbb{F}_2^N$, and $G_N \in \mathbb{F}_2^{N\times N}$ denote the codeword vector, information (or input) vector, and generator matrix, respectively.

The generator matrix is formulated as

$$G_N = G_2^{\otimes n}, \quad G_2 = \begin{pmatrix} 1 & 0 \\ 1 & 1 \end{pmatrix}, \tag{1}$$

where $n = \log_2 N$ and $G_2^{\otimes n}$ is the nth Kronecker power of G_2. As a result of encoding, the mutual information of transmitted bits (or bit channels) asymptotically approaches either 0 or 1 as N increases. Based on this phenomenon called *channel polarization*, polar codes select the most reliable K channels out of N channels, and information bits $v_1^K = (v_1, \ldots, v_K) \in \mathbb{F}_2^K$ are allocated only to these selected bit positions. The remaining $N - K$ bits are not used for information transmission, i.e., chosen as *frozen bits* whose values are known by the receiver *a priori*. Thus, the code rate of polar codes is $R = K/N$.

We denote $\mathcal{A}$ and $\mathcal{F}$ as the sets of information bit indices and frozen bit indices, respectively, where $\mathcal{A}, \mathcal{F} \subset \mathbb{N}$. It follows that $|\mathcal{A}| = K$ and $|\mathcal{F}| = N - K$, where $|\mathcal{I}|$ denotes the cardinality of a set $\mathcal{I}$.

B. SC DECODER AND SCL DECODER

We assume that each coded bit is transmitted by BPSK symbol with symbol energy E_s over an AWGN channel with the noise variance given by $N_0/2$. Let $y_1^N = (y_1, \ldots, y_N)$ denote the received symbol corresponding to the codeword x_1^N, and let $\hat{u}_1^N = (\hat{u}_1, \ldots, \hat{u}_N)$ denote the estimated input vector. (We also implicitly assume that the bit permutation has been applied to the encoder [8] such that the decoding of input bits is performed in the order of $\hat{u}_1, \hat{u}_2, \ldots, \hat{u}_N$).

SC decoder successively decodes each estimated input bit $\hat{u}_m$ with $m \in \{1, \ldots, N\}$. Let the log-likelihood ratio (LLR) of the mth bit channel of polar codes at the kth level of SC decoder be denoted by $L_k^{(m)}(y_1^N)$ for $k \in \{0, 1, 2, \ldots, n\}$, where $L_0^{(m)}(y_1^N) \equiv L_0^{(m)}(y_m)$ corresponds to the LLR of the received symbol y_m. If $\hat{u}_m$ corresponds to a frozen bit, then it is decoded as its predetermined value. Otherwise, it is decoded based on its corresponding LLR of the mth input bit at the nth level, i.e., $L_n^{(m)}(y_1^N)$, which is calculated as

$$L_n^{(m)}\left(y_1^N\right) = \begin{cases} \log \dfrac{P(y_1^N|u_m=0)}{P(y_1^N|u_m=1)}, & m = 1, \\ \log \dfrac{P\left(y_1^N, \hat{u}_1^{m-1}|u_m=0\right)}{P\left(y_1^N, \hat{u}_1^{m-1}|u_m=1\right)}, & m = 2, 3, \ldots, N, \end{cases} \tag{2}$$

and $\hat{u}_m$ is determined as

$$\hat{u}_m = \begin{cases} 0, \text{ if } L_n^{(m)}\left(y_1^N\right) \geq 0, \\ 1, \text{ otherwise.} \end{cases} \tag{3}$$

Finally, the estimated information bits $\hat{v}_1^K = (\hat{v}_1, \ldots, \hat{v}_K) \in \mathbb{F}_2^K$ are retrieved from $\hat{u}_1^N$ with $\mathcal{A}$.

Note that the LLR $L_k^{(m)}(y_1^N)$ can be recursively calculated for each level $k \in \{1, 2, \ldots, n\}$ and each stage $m \in \{1, 2, \ldots, N\}$ from the LLRs of the received symbols $\{L_0^{(1)}(y_1), L_0^{(2)}(y_2), \ldots, L_0^{(N)}(y_N)\}$ because of the unique structure of SC decoder. At each stage of decoding process by SC decoder, only a single candidate of decoded bits is stored, and the LLRs are calculated based on the previously decoded input bit sequence $\hat{u}_1^{m-1}$ for $m \geq 2$. As a result, this decoding process has a time and space complexity of $\mathcal{O}(N \log N)$, but it suffers from performance degradation associated with error propagation compared to the optimal (maximum-likelihood) decoding.

In contrast, SCL decoder stores up to L candidates of the information bit sequence, where L corresponds to the list size. At each decoding stage, SCL decoder calculates the path metrics that represent the reliability of the corresponding candidates. If the number of candidates exceeds L, those with lower path metrics are pruned. This expansion of search space improves the performance of SCL decoder as the list size L increases. The path metrics are calculated at each stage recursively based on the previous ones. In addition, it can be implemented on hardware using log-likelihood expression that enhances hardware efficiency [30]. However, the time complexity of SCL decoder increases, given by $\mathcal{O}(LN \log N)$ [9]. As a result, there is a trade-off between the reliability and decoding complexity of SCL decoder.

C. CRC-AIDED SCL DECODING

The performance of SCL decoder can be improved if it is concatenated by the error detector such as CRC codes [9]. The resulting decoder is often called CRC-aided SCL (CA-SCL) decoder [31]. This method employs a CRC code as an outer code and polar code as an inner code. By encoding information bits by CRC code before polar encoding, the performance of SCL decoder can be further improved. At the receiver side, in the process of SCL decoding, the most-reliable path that succeeds the CRC test is output. If all paths fail in the CRC test, it indicates that the decoder has failed to find the correct information vector.

D. SEGMENTED CRC-AIDED SCL DECODING

A decoding scheme called segmented CRC-aided SCL (SCA-SCL) decoding has been proposed in [15], which partitions the information bits into S *segments*. Each *segment* is separately encoded by a CRC code, and the resulting bit sequence is polar encoded and transmitted. At the receiver side, the received bits are decoded by SCA-SCL decoder, which repetitively applies CA-SCL decoding process to each segment in a successive manner. At the end of each CA-SCL decoding process, SCL decoder prunes the paths that have failed in the CRC test. A similar technique is proposed in [16], which leads to the reduction of space complexity with negligible performance loss. While each segment and CRC bits have equal lengths in [15], more general unequal cases are studied in [32], where it has been found that this unequal segmentation may improve the performance of decoder if properly designed.

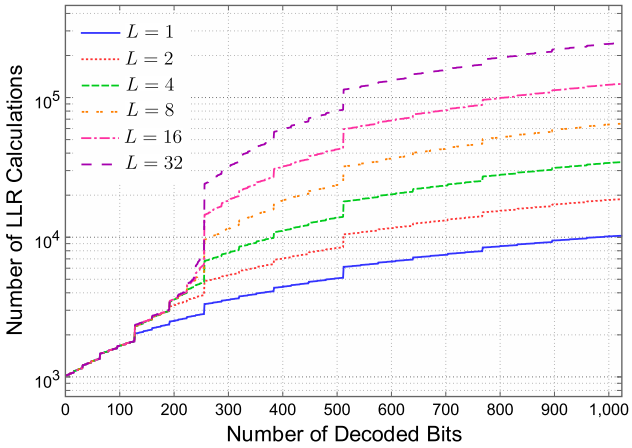

FIGURE 1. The cumulative number of LLR calculations required to decode each additional bit for the polar code with $N = 1024$.

III. PRIORITY-ORIENTED POLAR CODE

SC decoder can be implemented with low complexity, and SCL decoder can further enhance the performance with increasing complexity. However, these decoders based on successive cancellation may hinder its application to low-latency communications due to their decoding delay. To cope with this issue, we introduce a new polar decoding architecture, referred to as a *priority-oriented polar code* (POPC), which takes into account both reliability and decoding latency. Our approach exploits some structural properties of polar codes as well as the conventional SC and SCL decoders in terms of their reliability and decoding latency.

A. DECODING COMPLEXITY OF POLAR CODES

For SC and SCL decoding, the time complexity is dominated by the LLR update for each input bit [8], [9]. The number of LLR calculations is determined by the structure of polar codes. Based on the expression developed later in Section IV-D, Fig. 1 compares the cumulative number of LLR calculations required to successively process each additional bit of the polar code with codeword length $N = 1024$ for SCL decoding with list size L, where the case with $L = 1$ corresponds to SC decoding. Note that the vertical axis of Fig. 1 is given in the logarithmic scale. It is apparent that the number of required LLR calculations by SCL decoder is approximately L times that of SC decoder. The entire decoding complexity is also affected by other factors such as metric sorting operations of complexity $\mathcal{O}(L \log L)$. Thus,

the required computations of SCL decoding should be even higher. Apparently, the information bits located earlier can be decoded with a relatively small amount of LLR calculations, thus leading to lower decoding latency.

The results in Fig. 1 are based on the original SC and SCL decoders. If the simplified SC decoder [10] or simplified SCL decoder [33] is applied, it should reduce the number of LLR calculations. The effects of computational reduction achieved by these schemes are complementary to our decoding architecture. However, this issue is beyond the scope of this work and thus will not be pursued further.

B. STRUCTURE OF PRIORITY-ORIENTED POLAR CODES

We now describe our proposed POPC data structure. The proposed POPC divides information bits of length K into the following two parts: *priority bit sequence* (PBS) and *regular bit sequence* (RBS). They are specified as follows:

- PBS is designed to achieve its BLER less than a target BLER $P^*_{\mathrm{BL,p}}$ at a specific (reference) channel SNR, with the information bit length K_{p}. Since it is output before the entire information bits are decoded, it leads to lower latency than the conventional polar codes. PBS will be useful for the applications that require high reliability and low latency (i.e., those rely on URLLC).
- The remaining information bits are defined as RBS of length $K_{\mathrm{r}} = K - K_{\mathrm{p}}$ with a target BLER $P^*_{\mathrm{BL,r}}$. It can be used for the purpose of improving the quality of transmitted multimedia data, among many other possible applications.

Fig. 2 shows the structure of K information bits which are encoded by POPC. Let $v_1^{K_{\mathrm{p}}} = (v_1, v_2, \ldots, v_{K_{\mathrm{p}}}) \in \mathbb{F}_2^{K_{\mathrm{p}}}$ and $w_1^{K_{\mathrm{r}}} = (w_1, w_2, \ldots, w_{K_{\mathrm{r}}}) \in \mathbb{F}_2^{K_{\mathrm{r}}}$ denote the information vectors corresponding to PBS and RBS, respectively. As shown in Fig. 2(a), through POPC encoder, the elements in the vector $v_1^{K_{\mathrm{p}}}$ are mapped onto the head part of information bit channels of u_1^N such that they are decoded earlier than the remaining bits $w_1^{K_{\mathrm{r}}}$. We will also consider the case where each of PBS and RBS is encoded by CRC codes with their parity bit lengths given by r_{p} and r_{r}, respectively, as shown in Fig. 2(b). We denote the CRC parity bit vectors of PBS and RBS by $p_1^{r_{\mathrm{p}}} = (p_1, p_2, \ldots, p_{r_{\mathrm{p}}}) \in \mathbb{F}_2^{r_{\mathrm{p}}}$ and $q_1^{r_{\mathrm{r}}} = (q_1, q_2, \ldots, q_{r_{\mathrm{r}}}) \in \mathbb{F}_2^{r_{\mathrm{r}}}$, respectively. Note that this is equivalent to the information bit sequence structure adopted by SCA-SCL decoding with two segments ($S = 2$).

C. RECEIVER MODEL FOR PRIORITY ORIENTED POLAR CODES

Throughout this paper, we consider a binary-input additive white Gaussian noise (BI-AWGN) channel. At the receiver side, depending on the type of the adopted decoding scheme, different operation is performed. We propose the following three different types of decoders for POPC. Their detailed design guidelines are described in Section IV.

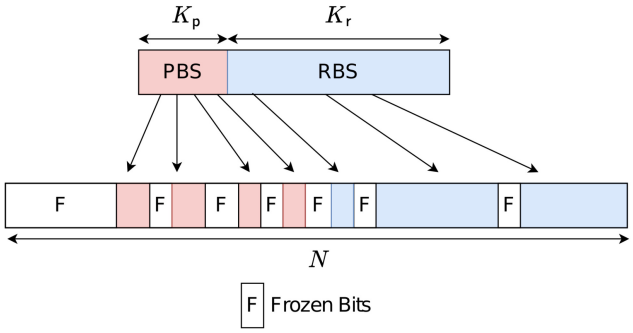

(a) Priority-oriented polar codes without CRC bits.

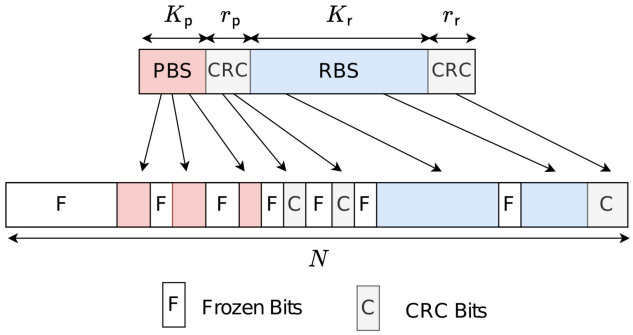

(b) Priority-oriented polar codes with CRC bits.

FIGURE 2. The structure of priority-oriented polar codes.

1) SC-BASED POPC DECODER

At first, we propose a POPC decoder based on the conventional SC decoding. In this case, only a single candidate of the decoded information bit sequence is stored. This means that once a bit in the information bit sequence is decoded, it will not be affected by the subsequent decoding process. Because of this decoding structure, PBS can be extracted immediately after the corresponding decoding process completes, without any loss of decoding performance compared to the conventional SC decoding. The resulting SC-based POPC decoder is shown in Fig. 3(a), where $\hat{v}_1^{K_{\mathrm{p}}}$ and $\hat{w}_1^{K_{\mathrm{r}}}$ correspond to the estimates of the CRC parity bit vectors $v_1^{K_{\mathrm{p}}}$ and $w_1^{K_{\mathrm{r}}}$, respectively.

2) SCL-BASED POPC DECODER

Unlike SC decoder, SCL decoder stores up to L paths of information bit sequences. This structure indicates that there are up to L candidates of PBS to be extracted from the decoder at each decoding stage. In contrast to SC decoding, the most important aspect of SCL decoding is that the best (partial) information bit sequence may be replaced by another candidate as decoding proceeds, and thus making decision earlier does not always result in most reliable decision, as will be discussed in Section IV. Based on this observation, we describe our SCL-based POPC decoder as follows: When the number of decoded information bits reaches the predetermined threshold K'_{p} (with $K'_{\mathrm{p}} \geq K_{\mathrm{p}}$), the

decoder outputs the most reliable path based on the path metrics. Our proposed system with SCL-based decoding has some similarity with that based on PSCL decoding [14] in that it outputs only a single path in the middle of SCL decoding, but the critical difference is that we output PBS only after additional decoding of subsequent information bits has been processed for improvement of its reliability.

How to determine the value K'_{p} will be discussed in Section IV. Note that RBS will be extracted from the decoder at the final decoding stage, which is the same as the conventional SCL decoder. The resulting SCL-based POPC decoder is shown in Fig. 3(b).

3) SCA-SCL-BASED POPC DECODER

Unlike SC-based decoder, SCL-based POPC decoder should output PBS several stages later for improved performance. On the other hand, as will be discussed in Section IV, if CRC code of proper length is concatenated with PBS, it can achieve the best BLER performance as long as it succeeds in the CRC test even if it is output from the decoder immediately after this test. Based on this property, POPC decoder can be implemented in a similar manner to the conventional SCA-SCL decoder in [15]. The resulting SCA-SCL-based POPC decoder is shown in Fig. 3(c), where $\hat{p}_1^{r_{\mathrm{p}}}$ and $\hat{q}_1^{r_{\mathrm{r}}}$ correspond to the estimates of $p_1^{r_{\mathrm{p}}}$ and $q_1^{r_{\mathrm{r}}}$, respectively.

IV. THEORETICAL ANALYSIS AND DESIGN GUIDELINE

In this section, we theoretically analyze the performance of the proposed POPC system and provide its design guideline considering specific decoder operations employed at the receiver.

Throughout this section, we adopt the following notations from [34]: We denote $\mathcal{A}_i$, $i \in \mathbb{N}$, as the subset of the information bit indices $\mathcal{A}$ that consists of the indices with i lowest values. In other words, $\mathcal{A}_i$ contains the first i information bit indices that will be decoded with lowest delay and thus $|\mathcal{A}_i| = i$. Also, the random variable is given by the capital letter, whereas the corresponding small letter represents its realization. Therefore, the random sub-vector corresponding to the realization $x_j^k = (x_j, \ldots, x_k)$ is denoted by $X_j^k = (X_j, \ldots, X_k)$.

A. POPC WITH SC-BASED DECODER

We first consider the case where the receiver employs the low complexity SC decoding shown in Fig. 3(a). In this case, the transmitter divides the information vector according to the two segments based on their importance as sketched in Fig. 2(a).

1) TRADE-OFF BETWEEN PBS SIZE AND BLER

The BLER of SC decoding can be estimated if the distributions of LLRs of the bit channels specified by $\mathcal{A}$ are known. Under the assumption that the all zero codeword is transmitted, the bit error probability of the mth input bit,

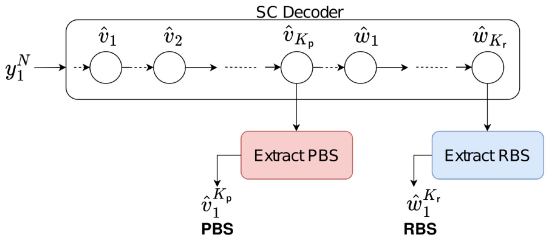

(a) SC-based POPC decoder.

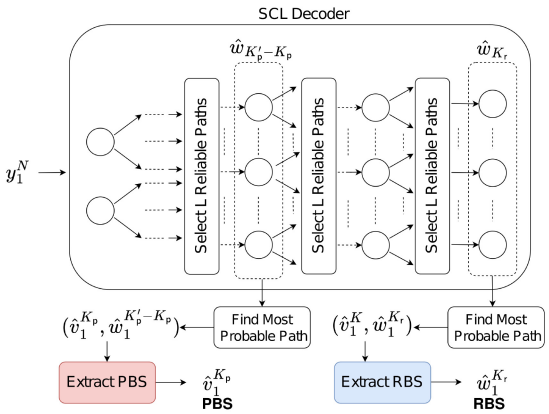

(b) SCL-based POPC decoder.

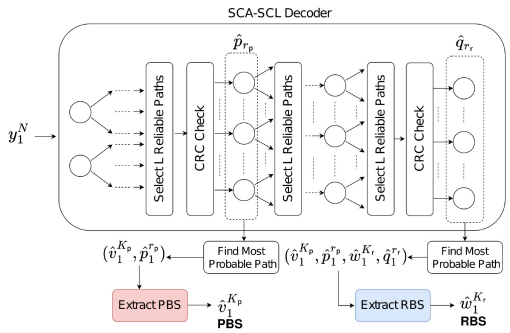

(c) SCA-SCL based POPC decoder.

FIGURE 3. Description of POPC decoding structure depending on the adopted base decoder. The nodes corresponding to the frozen bits are omitted for simplicity.

provided that all the previous bits are decoded correctly, can be expressed as

$$\begin{aligned} P_{\mathrm{b},m} &= P\big(\hat{u}_m \neq 0 \,|\, \hat{u}_1 = \cdots = \hat{u}_{m-1} = 0\big) \\ &= P\Big(L_n^{(m)}\Big(y_1^N\Big) < 0\Big). \end{aligned} \tag{4}$$

The BLER can be expressed as

$$P_{\mathrm{BL}} = 1 - \prod_{m \in \mathcal{A}} \big(1 - P_{\mathrm{b},m}\big). \tag{5}$$

In a similar manner, the BLER of PBS decoded by SC decoder can be expressed as

$$P_{\mathrm{BL,p}} = 1 - \prod_{m \in \mathcal{A}_{K_{\mathrm{p}}}} \big(1 - P_{\mathrm{b},m}\big). \tag{6}$$

Since $\mathcal{A}_{K_\mathsf{p}} \subset \mathcal{A}$, it follows that $P_{\mathrm{BL},\mathsf{p}} \leq P_{\mathrm{BL}}$. One can easily see that reducing K_p will thus result in reduced BLER according to (6).

Note that the distribution of LLR of the bit channels is often approximated by Gaussian, i.e., $L_k^{(m)}(y_1^N) \sim \mathcal{N}(\gamma_k^{(m)}, 2\gamma_k^{(m)})$ for $k \in \{1, 2, \ldots, n\}$ and $m \in \{1, 2, \ldots, N\}$, where $\gamma_k^{(m)}$ is the channel SNR corresponding to the mth bit channel of polar codes at the kth level of SC decoder. With this assumption, $P_{\mathrm{b},m}$ of (4) is approximated as

$$P_{\mathrm{b},m} \approx Q\left(\sqrt{\frac{\gamma_n^{(m)}}{2}}\right), \tag{7}$$

where $Q(x) \triangleq \frac{1}{2}\mathrm{erfc}(x/\sqrt{2})$.

2) DESIGN GUIDELINE FOR PBS LENGTH

Let $P^*_{\mathrm{BL},\mathsf{p}}$ denote the target maximum BLER acceptable for PBS. For a given channel SNR γ, we wish to maximize K_p under this BLER constraint. It can easily be found by testing $P_{\mathrm{BL},\mathsf{p}}$ for a given value of K_p through Monte-Carlo simulations or the above analysis based on Gaussian approximation. One may then select the maximum K_p that satisfies the condition of $P_{\mathrm{BL},\mathsf{p}} \leq P^*_{\mathrm{BL},\mathsf{p}}$.

B. POPC WITH SCL-BASED DECODER

Following the modeling of [34], we regard the input vector (including frozen bits) as a random vector expressed by $U_1^N = (U_1, U_2, \ldots, U_N)$, with its realization $u_1^N = (u_1, u_2, \ldots, u_N)$.

In what follows, we use the notation $U_\mathcal{I}$ to denote a random sub-vector of U_1^N with its components selected according to a given index set $\mathcal{I} \subset \mathbb{N}$.

1) RELATIONSHIP BETWEEN PBS SIZE AND DECODING PERFORMANCE

In [34], the performance of SCL decoding has been analyzed from an information-theoretic perspective. We analyze the relationship between the error rate performance of PBS and its size based on the approach of [34].

Let us write a set of the smallest natural numbers of size m as $[m] = \{1, 2, \ldots, m\}$. We define $\mathcal{A}^{(m)} \triangleq \mathcal{A} \cap [m]$ and $\mathcal{F}^{(m)} \triangleq \mathcal{F} \cap [m]$, i.e., $\mathcal{A}^{(m)}$ and $\mathcal{F}^{(m)}$ are the sets of the information and frozen bit indices observed in the first m input bits to SCL decoder, respectively.

Suppose that decoding of the first m input bits is complete. In this case, given the observation of the received random vector $Y_1^N = y_1^N$, we know the frozen bits $U_{\mathcal{F}^{(m)}}$ by assumption, but the information bits $U_{\mathcal{A}^{(m)}}$ are unknown. Therefore, in [34], the uncertainty measure within the first m input bits during SCL decoding is defined as

$$d_m\left(y_1^N\right) \triangleq H\left(U_{\mathcal{A}^{(m)}} \mid Y_1^N = y_1^N, U_{\mathcal{F}^{(m)}}\right). \tag{8}$$

If the realization of the received random vector Y_1^N is not given, then $d_m(y_1^N)$ can be a random variable, which we denote by D_m. The expected value of D_m, denoted by $\bar{D}_m$, corresponds to the conditional entropy given by

$$\bar{D}_m \triangleq \mathbb{E}\left[d_m\left(Y_1^N\right)\right] = H\left(U_{\mathcal{A}^{(m)}} \mid Y_1^N, U_{\mathcal{F}^{(m)}}\right). \tag{9}$$

If U_m is an information bit, then, by the chain rule, we have

$$\bar{D}_m = \bar{D}_{m-1} + H\left(U_m \mid Y_1^N, U_1^{m-1}\right). \tag{10}$$

On the other hand, if U_m is a frozen bit, then we have

$$\begin{aligned}\bar{D}_m = \bar{D}_{m-1} &+ H\left(U_m \mid Y_1^N, U_1^{m-1}\right) \\ &- H\left(U_m \mid Y_1^N, U_{\mathcal{F}^{(m-1)}}\right).\end{aligned} \tag{11}$$

Therefore, $\bar{D}_m$ is expressed as

$$\begin{aligned}\bar{D}_m = &\sum_{j \in \mathcal{A}^{(m)}} H\left(U_j \mid Y_1^N, U_1^{j-1}\right) \\ &- \sum_{j \in \mathcal{F}^{(m)}} \left\{H\left(U_j \mid Y_1^N, U_{\mathcal{F}^{(j-1)}}\right) - H\left(U_j \mid Y_1^N, U_1^{j-1}\right)\right\}.\end{aligned} \tag{12}$$

The above equation shows that since the frozen bits are completely random by assumption, knowing them will reduce the uncertainty of the information bits, whereas decoding information bits will increase the uncertainty, which agrees with the observation of the performance of SC decoder in the previous subsection. Since $H(U_j \mid Y_1^N, U_{\mathcal{F}^{(j-1)}}) \leq 1$, $\bar{D}_m$ can be lower bounded as

$$\begin{aligned}\bar{D}_m \geq &\sum_{j \in \mathcal{A}^{(m)}} H\left(U_j \mid Y_1^N, U_1^{j-1}\right) \\ &- \sum_{j \in \mathcal{F}^{(m)}} \left(1 - H\left(U_j \mid Y_1^N, U_1^{j-1}\right)\right) \triangleq \bar{D}_m^{\mathrm{LB}}.\end{aligned} \tag{13}$$

Note that if U_j is an information bit, then we may express

$$H\left(U_j \mid Y_1^N, U_1^{j-1}\right) = H_2(P_{\mathrm{b},j}), \tag{14}$$

where $H_2(p) = -p\log_2 p - (1-p)\log_2(1-p)$ is the binary entropy function, and $P_{\mathrm{b},j}$ is the bit error probability of the jth bit defined by (4). Note also that when we select m such that $|\mathcal{A}^{(m)}| = K_\mathsf{p}$, $\bar{D}_m$ corresponds to the conditional entropy of PBS in our system model.

To investigate the effectiveness of the above argument, we simulate a polar code with $N = 1024$ and $K = 512$, where the code is designed using reciprocal channel approximation (RCA) algorithm described in [35] with the design SNR of -1.5 dB.[2] The received symbol vector is decoded by SCL decoder with list size $L = 16$. The resulting BLER, $P_{\mathrm{BL},\mathsf{p}}$, with respect to the size of PBS, K_p, measured at the channel SNR of $E_s/N_0 = -1.5$ dB is plotted in Fig. 4.

[2]There have been several low complexity polar code construction algorithms developed in the literature, such as Gaussian approximation (GA) [36] and improved GA [37]. It has been demonstrated in [35] that RCA can more accurately estimate the SNR of the input bit channels than GA and improved GA. Therefore, we adopt RCA throughout this work.

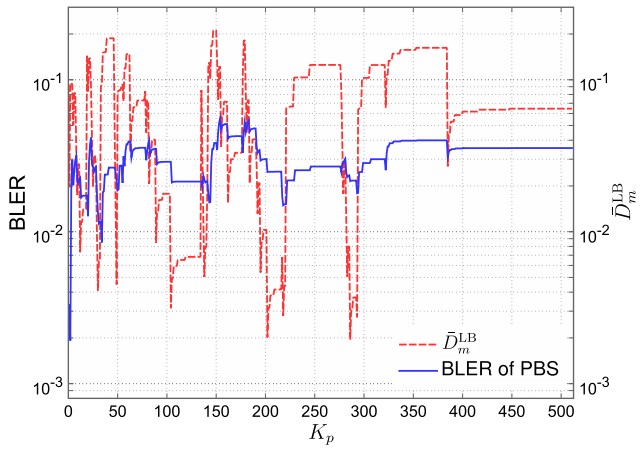

FIGURE 4. BLER of PBS $P_{\mathrm{BL,p}}$ in a rate-1/2 polar code decoded by SCL decoding of list size $L = 16$, with respect to the size of PBS. Also shown is the value of the corresponding conditional entropy lower bound $\bar{D}_m^{\mathrm{LB}}$. Note that the tick labels of BLER are on the left hand side, whereas those of $\bar{D}_m^{\mathrm{LB}}$ are on the right hand side.

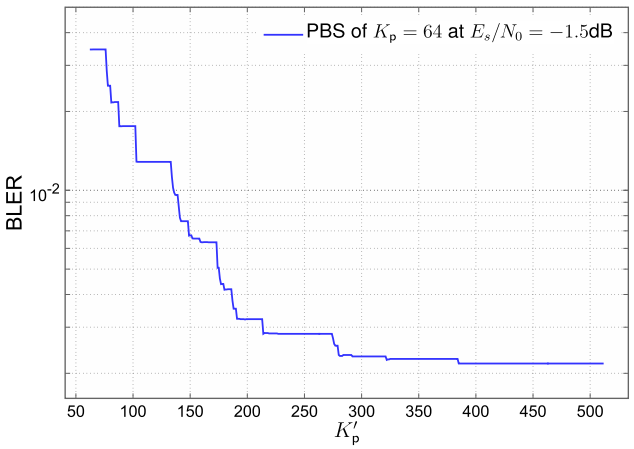

FIGURE 5. BLER of PBS with size $K_{\mathrm{p}} = 64$ by SCL decoder of $L = 16$ with respect to the window size K'_{p} for the range of $K_{\mathrm{p}} \le K'_{\mathrm{p}} \le K$.

Also shown is the analytical value of $\bar{D}_m^{\mathrm{LB}}$ expressed in (13) with the bit error probability $P_{\mathrm{b},j}$ calculated according to (7), where the SNR of the bit channel is also calculated by RCA. Even though the scales of $P_{\mathrm{BL,p}}$ and $\bar{D}_m^{\mathrm{LB}}$ are different, we observe the same tendency in that when SCL decoder processes the information bits, both the simulated BLER and analytically calculated value of $\bar{D}_m^{\mathrm{LB}}$ increase similar to SC decoding, whereas they both decrease when the decoder processes the frozen bits. This clearly demonstrates that unlike SC decoder, BLER values fluctuate depending on the size of PBS in the case of SCL decoder.

2) BLER OF PBS WITH RESPECT TO WINDOW SIZE

So far, we have observed that BLER of PBS processed by SCL decoding exhibits some fluctuation depending on its length, whereas it will almost monotonically increase with its length in the case of SC decoding.

In what follows, we show that BLER of PBS is likely to improve if we increase the window size K'_{p} ($K'_{\mathrm{p}} \ge K_{\mathrm{p}}$) that determines the timing when the estimated PBS of size K_{p} is output from the decoder. To this end, we investigate the conditional entropy of PBS with respect to the timing (or window size) K'_{p} when the sequence is output from the decoder.

Suppose that the number of decoded information bits in PBS reaches K_{p} at the mth decoding stage. If PBS is output from the decoder immediately after its decoding process, the conditional entropy of PBS is given by $\bar{D}_m = H(U_{\mathcal{A}^{(m)}} \mid U_{\mathcal{F}^{(m)}}, Y_1^N)$. Similarly, let the conditional entropy of PBS that is output from SCL decoder later, i.e., at the m'th decoding stage with $m' > m$, denote

$$\bar{D}_m^{(m')} \triangleq H\left(U_{\mathcal{A}^{(m)}} \mid U_{\mathcal{F}^{(m')}}, Y_1^N\right). \tag{15}$$

Then we have the following theorem:

Theorem 1: For increasing m' with $m' > m$, $\bar{D}_m^{(m')}$ is monotonically non-increasing.

Proof: Since $U_{\mathcal{F}^{(m)}} \subset U_{\mathcal{F}^{(m')}}$ and conditioning could reduce but does not increase the entropy, we have $\bar{D}_m^{(m')} \le \bar{D}_m$. ■

The above theorem implies that PBS output by SCL decoder at later decoding stage may not degrade but possibly improve the resulting decoding performance.

To see if the above argument holds in practice, Fig. 5 shows the simulated BLER of PBS with respect to the window size K'_{p}, where the size of PBS is fixed as $K_{\mathrm{p}} = 64$ and SCL is applied with list size $L = 16$. (The other parameters are the same as those shown in Fig. 4.) As observed, BLER of PBS tends to decrease as K'_{p} increases. Furthermore, it approaches a certain lower limit as the SCL decoding stage proceeds. This indicates that there is a suitable limiting value of K'_{p} beyond which BLER will no longer improve.

3) DESIGN GUIDELINE

Unlike SC decoding, estimation of decoding performance for SCL is challenging in general due to its complexity that grows exponentially with the information length. We thus propose to specify the size of PBS K_{p} in advance and heuristically determine the smallest window size at which PBS can achieve the target BLER.

Specifically, let $P^*_{\mathrm{BL,p}}$ denote the target maximum BLER acceptable for PBS. For a given channel SNR γ and K_{p}, we simulate BLER $P_{\mathrm{BL,p}}$ with respect to the window size K'_{p}. We then select the minimum K'_{p} that satisfies the condition of $P_{\mathrm{BL,p}} \le P^*_{\mathrm{BL,p}}$. In this manner, the latency of SCL decoder for PBS can be minimized while achieving the required reliability.

C. DECODING BY SCA-SCL-BASED POPC DECODER

When CRC code is concatenated with PBS, its decoding performance improves even if PBS is output immediately after decoding with CRC test, similar to the conventional CA-SCL decoder. In this subsection, we analyze the error

performance of SCA-SCL-based POPC decoder based on the approach in [38], [39].

1) BLER ESTIMATION

In [38], [39], an approximate upper bound on the error probability of CA-SCL decoding has been derived provided that BLER of the conventional SCL decoding is given in advance. We denote the BLER of CA-SCL decoder by $P_{\mathrm{BL}}(\gamma, L)$, where L is the list size of SCL decoder and γ is the channel SNR. Let l^* represent the list index corresponding to the correct codeword, and r denote the length of CRC bits. For simplicity, we assume that the list indices are sorted such that paths with smaller list indices correspond to more likely candidates. If no correct codeword exists in the list, we assume $l^* > L$.

Given the assumption that the correct codeword in the list can be detected by CRC without error, the ideal decoding error probability $P_{\mathrm{BL,id}}(\gamma, L)$ can be defined as

$$P_{\mathrm{BL,id}}(\gamma, L) \triangleq 1 - \sum_{l=1}^{L} P_{l^*}(\gamma, l), \tag{16}$$

where $P_{l^*}(\gamma, l)$ denotes the probability that the lth path corresponds to the codeword correctly decoded by SCL decoder (i.e., $l^* = l$), for a given channel SNR γ over an AWGN channel.

In practice, however, error detection of the correct codeword by CRC test may fail. Taking this effect into account, the approximate upper bound of the decoding error probability is given by [38], [39]

$$\begin{aligned} P_{\mathrm{BL}}(\gamma, L) &\lesssim 1 - \sum_{l=1}^{L} P_{l^*}(\gamma, l)\left\{1 - (l-1)2^{-r}\right\} \\ &= P_{\mathrm{BL,id}}(\gamma, L) + 2^{-r} \sum_{l=2}^{L} P_{l^*}(\gamma, l)(l-1). \end{aligned} \tag{17}$$

From (17), we observe that BLER of CA-SCL decoding can approach the ideal decoding error probability $P_{\mathrm{BL,id}}(\gamma, L)$ when the length of CRC code is sufficient (i.e., as $r \to \infty$) as expected.

The above mathematical expression can be used to assess the performance of PBS. Contrary to the original CA-SCL decoding method, which computes the decoding error distribution $P_{\mathrm{BL}}(\gamma, L)$ at the end of SCL decoding process, we calculate the BLER of PBS with $P_{l^*}(\gamma, L)$ at the $(K_{\mathsf{p}} + r_{\mathsf{p}})$th decoding stage (i.e., when the decoding process of the first segment completes). As mentioned in the previous subsection, the calculation of $P_{l^*}(\gamma, l)$ in (16) and (17) through theoretical analysis is computationally challenging. Therefore, we resort to Monte-Carlo simulations for its estimation. As a result, we refer to the corresponding BLER evaluation approach based on (17) with simulated values of $P_{l^*}(\gamma, l)$ as *hybrid analysis* in what follows. The BLER calculation based on the conventional simulation will be referred to as *full simulation* accordingly.

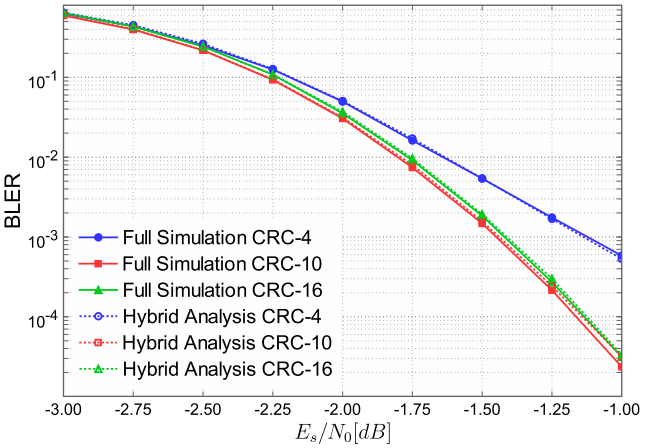

FIGURE 6. Comparison of BLER based on full simulation and hybrid analysis for PBS of $K_{\mathsf{p}} = 64$ decoded using CA-SCL decoding with $L = 16$ and CRC lengths of $r_{\mathsf{p}} = 4$, 10, and 16.

TABLE 2. A list of adopted CRC polynomials.

Degree of CRC polynomial	CRC polynomial (Hexadecimal)
4	0x9
10	0x327
16	0x8810 [40]
24	0xc3267d [41]
40	0x80000000f3

In Fig. 6, we evaluate the BLER performance of PBS in the proposed scheme employing several different values of CRC length r_{p}. The codeword length is chosen to be $N = 1024$, and the codes are constructed by RCA algorithm with a design SNR of -1.0 dB. The total length of information bits and CRC parity bits is fixed as $K + r_{\mathsf{p}} + r_{\mathsf{r}} = 512$, and the size of PBS is chosen to be $K_{\mathsf{p}} = 64$. Since K_{p} and $K + r_{\mathsf{p}} + r_{\mathsf{r}}$ are kept constant in this comparison, increasing r_{p} results in reduced K_{r} in this system. Note also that the SNR is not affected by the length of r_{p}, since the SNR is defined here as the ratio of the transmit symbol power to the noise power. The results are shown for a list size of $L = 16$, with $r_{\mathsf{p}} = 4$, 10, and 16, where the CRC polynomials employed here are listed in Table 2.

We note that the case of hybrid analysis in Fig. 6 does not require any CRC operation, i.e., simply the evaluation by the conventional SCL decoding through Monte-Carlo simulation suffices. On the other hand, the corresponding *full* simulation results shown in Fig. 6 are based on the actual BLER evaluation by counting the block error events *with a given CRC*, which is more time-consuming in general. From Fig. 6, we observe that the results based on hybrid analysis and full simulation match well, justifying our evaluation in terms of the different CRC lengths.

2) RELATIONSHIP BETWEEN PBS SIZE AND DECODING PERFORMANCE

When the length of CRC is sufficient, one can assume that the performance of polar codes approaches the ideal BLER

defined in (16). In this case, the following theorem may hold:

Theorem 2: Let $P^{(i)}_{\mathrm{BL,id}}$ denote the ideal BLER of information bit sequence where the length of information bit sequence including CRC parity bits is i. Then $P^{(i)}_{\mathrm{BL,id}}$ is monotonically non-decreasing with i.

Proof: From (16), $P^{(i)}_{\mathrm{BL,id}}$ can be interpreted as the probability that the correct path exists in L paths at the ith decoding stage. We consider the following two cases: 1) If there is no correct path in all L paths at the ith stage, then there is no possibility that there exists the correct path at the $(i+1)$th stage. 2) Even if there exists the correct path among L paths at the ith stage, it may be possible that the correct path will be pruned in the $(i+1)$th stage. As a result, one may conclude that $P^{(i)}_{\mathrm{BL,id}} \leq P^{(i+1)}_{\mathrm{BL,id}}$. ■

The above theorem states that when PBS is concatenated with CRC of sufficient length such that all the incorrect paths in CA-SCL decoding should be identified perfectly, then BLER of PBS can be improved by reducing the length of PBS similar to that with SC decoding. In fact, we observe from Fig. 6 that BLER *improves* by increasing CRC lengths from 4 to 10 as it enhances the probability of identifying the incorrect paths, but BLER *degrades* by further increase of CRC length from 10 to 16 because of the above reason. This is in contrast to the system based on SCL decoding, where longer PBS does not always degrade its BLER performance as observed in Fig. 4.

3) DESIGN GUIDELINE

In the case of SCA-SCL-based decoding, the lengths of CRC for PBS and RBS, i.e., r_{p} and r_{r}, as well as their information bit lengths, K_{p} and K_{r}, should be appropriately designed.

We first focus on the design of PBS. Let $P^{*}_{\mathrm{BL,p}}$ denote the target maximum BLER acceptable for PBS. For a given channel SNR γ and K_{p}, we first determine the length of CRC based on (17). We set the minimum length of r_{p} such that $P_{\mathrm{BL}}(\gamma, L) - P_{\mathrm{BL,id}}(\gamma, L) < \epsilon$, where ϵ is a given parameter that corresponds to an acceptable gap between the ideal BLER and the actual BLER considering the effect of CRC. Note that from (17) we have

$$\epsilon \lesssim 2^{-r} \sum_{l=2}^{L} P_{l^*}(\gamma, l)(l-1). \tag{18}$$

The parameters K_{r} and r_{r} can be determined in the same manner for a given target maximum BLER $P^{*}_{\mathrm{BL,r}}$.

D. ANALYSIS OF DECODING COMPLEXITY FOR INFORMATION BIT SEQUENCE

Finally, we derive an expression for the number of LLR calculations required to decode the first m input bits of length-N polar code (with $N = 2^n$) by SCL decoder of list size L.

Let us consider decoding of the jth input bit u_j, where the corresponding LLR is expressed by $L^{(j)}_n(y_1^N)$ with reference to (2). Let $\ell \triangleq j-1 \in \{0, 1, \ldots, N-1\}$ and express its binary representation as $(b_1, b_2, \ldots, b_n)$. Let Z_ℓ denote the number of runs of 0 starting from the rightmost bit b_n in its binary representation. For example, if $n = 4$ and $j = 5$, then we have $\ell = 4$ and thus its binary representation is given by $(0, 1, 0, 0)$, leading to $Z_\ell = 2$. Due to the structure of polar codes, for the jth input bit, the number of LLRs that should be required for calculation is given by

$$\sum_{j=0}^{Z_\ell} 2^j = 2^{Z_\ell+1} - 1. \tag{19}$$

As a result, in the case of SC decoder, the total number of LLR calculations up to the first m input bits is given by

$$\sum_{k=1}^{m} \left(2^{Z_{k-1}+1} - 1\right). \tag{20}$$

In the case of SCL decoding, let L_k denote the maximum number of survival paths upon processing the kth input. With $L_1 = 1$, it can be recursively determined for $k > 1$ as

$$L_k = \begin{cases} L_{k-1}, & \text{if } k \notin \mathcal{A}, \\ \max(2L_{k-1}, L), & \text{if } k \in \mathcal{A}. \end{cases} \tag{21}$$

The resulting number of LLR calculations up to the first m input bits is given by

$$\sum_{k=1}^{m} L_k \left(2^{Z_{k-1}+1} - 1\right). \tag{22}$$

To evaluate the number of LLR calculations required for decoding PBS in our proposed architecture using (22), the number of input bits m should be set such that $|\mathcal{A}^{(m)}|$ is equal to K_{p}, K'_{p}, and $K_{\mathsf{p}} + r_{\mathsf{p}}$ in the case of our SC, SCL, and SCA-SCL-based decoding, respectively. Also, the results shown in Fig. 1 were calculated based on (22) as a function of the number of decoded input bits m.

V. NUMERICAL RESULT

In the following performance evaluations based on extensive simulations, we consider the scenario where the target BLERs of PBS and RBS are given by $P^{*}_{\mathrm{BL,p}} = 10^{-6}$ and $P^{*}_{\mathrm{BL,r}} \leq 10^{-5}$, respectively. We focus on the SNR range where these target values are achievable with proper design of parameters.

Throughout this section, we set the baseline polar code parameters as $N = 1024$ and $K = 512$, and the list sizes of SCL-based and SCA-SCL-based decoders are both chosen as $L = 16$.

A. DECODING BY SC-BASED DECODER

We first focus on the proposed POPC with SC-based decoding. In this case, we construct the polar code based on RCA algorithm [35] with given parameters of N and K. Through the BLER estimation according to (6) with (7), we may find that with design SNR of $E_s/N_0 = 0.74$ dB, we can achieve the target BLER of 10^{-5} in the conventional SC decoding. Therefore, we focus on BLER performance at the channel SNR equal to $E_s/N_0 = 0.74$ dB.

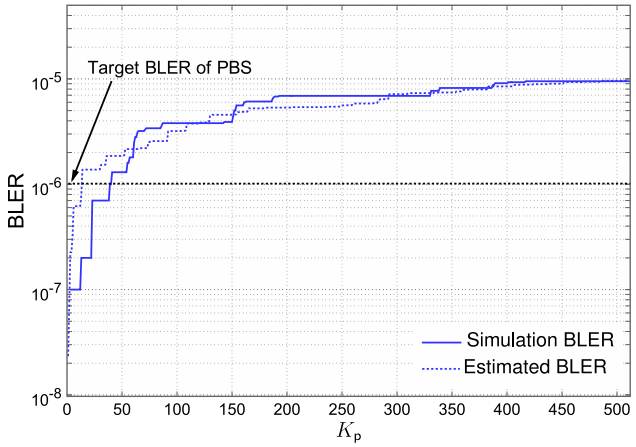

FIGURE 7. Comparison between simulated and estimated BLER for PBS with respect to its size, where the channel SNR and design SNR are both set as $E_s/N_0 = 0.74$ dB.

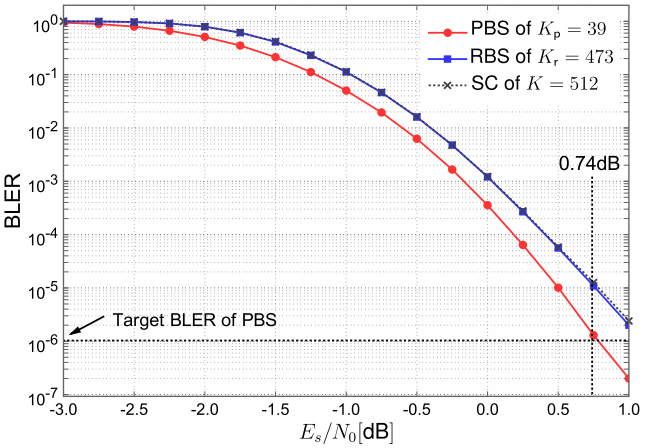

FIGURE 8. Simulation results of BLER performance for PBS of $K_p = 39$ and RBS of $K_r = 473$ decoded by SC-based decoder. BLER of the conventional SC decoder (with $K = 512$) is also shown for comparison.

1) DESIGN OF PBS

By Monte-Carlo simulation with $E_s/N_0 = 0.74$ dB, we generate a BLER curve as a function of PBS size K_p. The results are shown in Fig. 7, where the estimated BLER calculated from (6) is also plotted for comparison. From the results, PBS size that can achieve $P^*_{\mathrm{BL},p}$ is found to be $K_p = 39$ by simulation, whereas that based on the estimated BLER is around $K_p = 13$, which is considerably pessimistic compared to the simulated result. This difference may stem from the fact that the estimated theoretical BLER makes use of the assumption that LLR should follow Gaussian distribution, which may not be necessarily accurate when evaluating BLER values as low as 10^{-6}. Note that the two curves almost agree when we compare them at BLER of 10^{-5} achieved with $K_p \approx K = 512$.

2) BLER PERFORMANCE

Based on the result in Fig. 7, we set $K_p = 39$ in what follows. Fig. 8 shows BLER curves of PBS and RBS, where the size of RBS is $K_r = K - K_p = 473$. The case of the conventional SC decoder with $K = 512$ is also shown for comparison. From this figure, we observe that the performance of PBS is always better than that of RBS as expected, while both satisfying their respective target BLER values at the design SNR. The conventional SC decoder performs identical to RBS as expected, which indicates that early output of PBS does not affect the performance of the remaining bit sequence.

3) DECODING COMPLEXITY

In Table 3, the complexity required to decode PBS exclusively and the entire sequence with SC decoder is compared, where the complexity is defined as the number of required LLR calculations, expressed by (22), evaluated at the time when the corresponding sequence is extracted. It is shown that complexity of decoding PBS is about 40% compared to the conventional SC decoding applied to a single information sequence.

TABLE 3. Complexity of PBS and full sequence based on SC decoding.

	PBS	Full Sequence
Information Size	$K_p = 39$	$K = 512$
Complexity	4051	10240
Ratio	40%	

B. DECODING BY SCL-BASED DECODER

We next evaluate BLER of the proposed POPC with SCL decoding. We assume that the channel SNR is $E_s/N_0 = 0.48$ dB, and divide $K = 512$ into PBS and RBS of lengths $K_p = 64$ and $K_r = 448$, respectively. Polar code is constructed with RCA, where the design SNR is set equal to the above channel SNR.

1) DESIGN OF PBS

We first simulate the BLER curve $P_{\mathrm{BL},p}$ with respect to the window size K'_p of our SCL-based decoder, and the result is shown in Fig. 9, where we observe that BLER of PBS falls below its target $P^*_{\mathrm{BL},p} = 10^{-6}$ with $K'_p \approx 90$ and above. Thus, we set $K'_p = 90$ in what follows.

2) BLER PERFORMANCE

Fig. 10 shows the BLER performance of PBS with $K'_p = 90$ along with that of RBS. The case of PBS with $K'_p = K_p = 64$ is also shown as a reference, as well as that of the conventional SCL decoder with $K = 512$ for comparison. From this figure, we observe that the designed PBS achieves the target BLER at the channel SNR equal to the design SNR as expected. We also observe that the BLER performance of PBS with $K'_p = 90$ is superior to that with $K'_p = K_p$ in all SNR region, suggesting the importance of appropriate selection of the window size. It is interesting to note that even though PBS is superior to RBS in high SNR region, RBS outperforms PBS in low SNR region due to the effect of using longer window size. BLER of the conventional SCL decoder achieves almost the same performance as that of

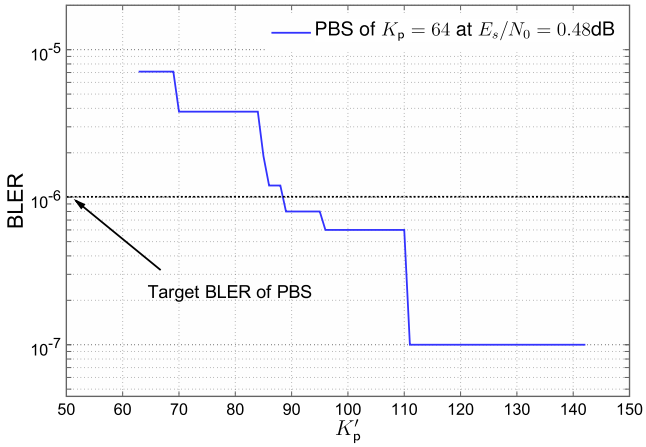

FIGURE 9. BLER of PBS decoded by SCL-based decoder ($L = 16$) with respect to the window size K'_p where the channel SNR and design SNR are both set as $E_s/N_0 = 0.48$ dB.

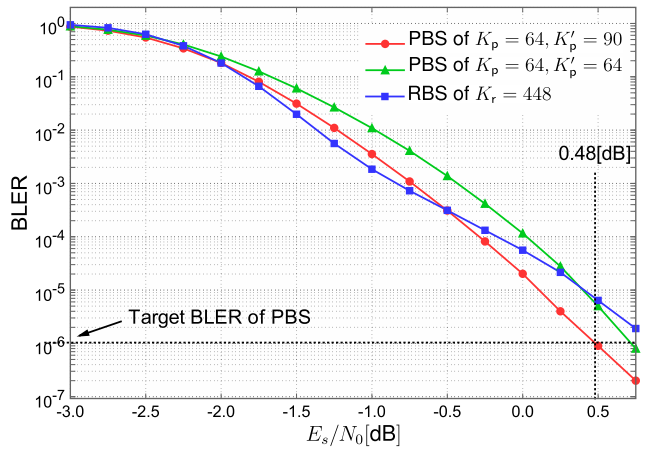

FIGURE 10. BLER performance of PBS of $K_\mathrm{p} = 64$ where the window sizes are $K'_\mathrm{p} = 90$ as well as $K'_\mathrm{p} = K_\mathrm{p}$, and that of RBS of $K_\mathrm{r} = 448$, all decoded by SCL-based decoder. BLER of the conventional SCL decoder (with $K = 512$) is also shown for comparison.

TABLE 4. Complexity of PBS and full sequence based on SCL decoding.

	PBS	Full Sequence
Information Size	$K_\mathrm{p} = 64$	$K = 512$
Window Size	$K'_\mathrm{p} = 90$	$K'_\mathrm{p} = K$
Complexity	39376	125904
Ratio	31%	

RBS, indicating that early output of PBS does not affect the performance of RBS.

3) DECODING COMPLEXITY

In Table 4, the complexity required to decode PBS exclusively and the entire sequence with SCL decoder is compared, where the complexity is defined as the number of LLR calculations given by (22) at the time when the corresponding sequence is extracted. It is shown that complexity of decoding PBS is about 31% compared to the conventional SCL decoding.

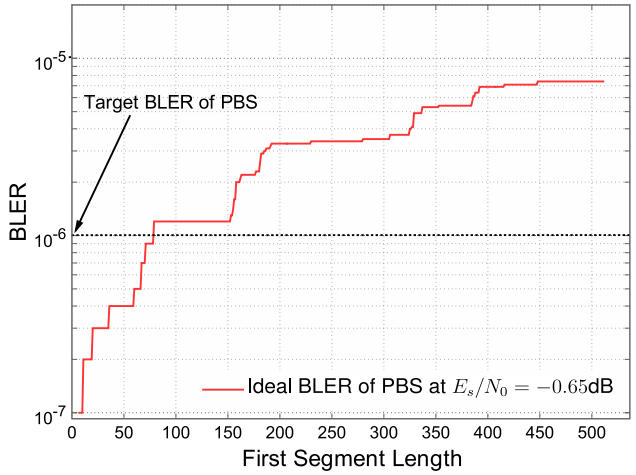

FIGURE 11. Ideal BLER for PBS with respect to the length of the first segment (including parity bits) decoded by SCA-SCL-based decoder, where the channel SNR and design SNR are both set as $E_s/N_0 = -0.65$ dB.

C. DECODING BY SCA-SCL-BASED DECODER

Finally, we investigate the performance of the proposed POPC with SCA-SCL-based decoder.

We wish to design the system such that the target BLER values can be achieved at the reference channel SNR of $E_s/N_0 = -0.65$ dB. Polar code is constructed based on RCA, where the design SNR is set equal to the reference channel SNR. Throughout this section, the total length of information bits and parity bits is fixed as $K + r_\mathrm{p} + r_\mathrm{r} = 512$.

1) DESIGN OF PBS

We first identify the size of PBS (including parity bits) that can achieve the target BLER value. Fig. 11 compares the ideal BLER $P_{\mathrm{BL,id}}(\gamma, L)$ with respect to the length of the first segment consisting of both PBS and CRC parity bits, i.e., $i_\mathrm{p} \triangleq K_\mathrm{p} + r_\mathrm{p}$. The result indicates that the BLER of PBS achieves the target value of $P^*_{\mathrm{BL,p}} = 10^{-6}$ when the size of the first segment is $i_\mathrm{p} = 79$. Here, the assumption is that CRC code can detect the error perfectly (i.e., with sufficient length of r_p).

Given the length of the first segment, we next determine the length of r_p that can achieve sufficiently low values of the gap ϵ expressed by (18). We have calculated ϵ by simulations to find that $r_\mathrm{p} = 16$ is large enough ($\epsilon \ll 10^{-6}$), which will be adopted in what follows.

2) BLER PERFORMANCE

We set the parity bit lengths of CRC codes for PBS and RBS as $r_\mathrm{p} = 16$ and $r_\mathrm{r} = 24$, respectively. Therefore, the sizes of PBS and RBS are given by $K_\mathrm{p} = 63$ and $K_\mathrm{r} = 409$, respectively. As a reference, we also evaluate the case of the conventional CA-SCL decoder with $K = 472$ and $r = 40$. Here, we select the length of CRC equal to the sum of r_p and r_r, which turns out to be large enough. We expect that reduction of CRC length may enhance the information rate slightly over the proposed system without noticeable performance degradation.

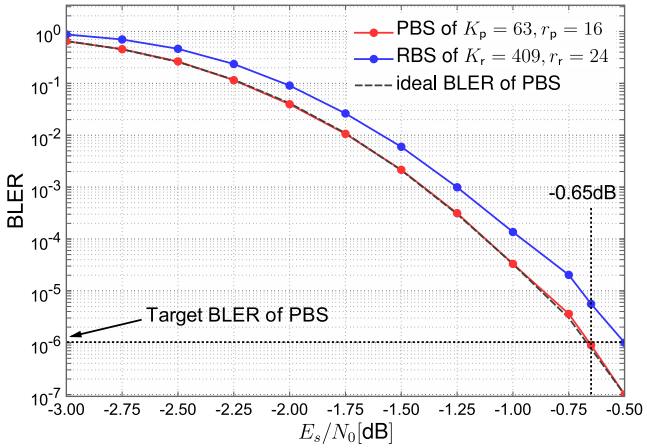

FIGURE 12. BLER performance of PBS of $K_p = 63$ and $r_p = 16$ and RBS of $K_r = 409$ and $r_r = 24$ with respect to the channel SNR for polar codes decoded by SCA-SCL-based decoder. BLER of the conventional CA-SCL decoder with $K = 472$ and $r = 40$ is also shown for comparison.

TABLE 5. Complexity of PBS and full sequence based on SCA-SCL decoding.

	PBS	Full Sequence
Information Size	$K_p + r_p = 79$	$K + r_p + r_r = 512$
Complexity	36760	125848
Ratio	29%	

Fig. 12 shows the BLER curves for PBS and RBS, as well as that of the conventional CA-SCL decoding, where all polar codes are constructed by RCA and the corresponding CRC polynomials adopted here are listed in Table 2. As a reference, the ideal BLER of PBS (achieved by CRC code of sufficient length) is also shown. From the result, We observe that the BLER curves of PBS and RBS achieve their respective target BLER values when evaluated at a given reference channel SNR as expected.

3) DECODING COMPLEXITY

In Table 5, the complexity required to decode PBS exclusively and the entire sequence with SCA-SCL-based decoder is compared, where the complexity is defined as the number of LLR calculations given by (22) at the time when the corresponding sequence is extracted. It is shown that complexity of decoding PBS is about 29% compared to the conventional SCA-SCL decoding.

VI. CONCLUSION

In this paper, we have introduced a new polar code architecture called POPC, which achieves high reliability and reduced latency for selected information bit sequence, and developed suitable encoding and decoding models for three different types of decoders (i.e., SC, SCL, and SCA-SCL). In addition, design guidelines for the lengths of PBS and RBS that can achieve their respective target BLER values have been presented according to each decoding scenario. The simulation results over a BI-AWGN channel have shown that both PBS and RBS can achieve their target BLER values at a given reference channel SNR. We have demonstrated that PBS can achieve higher reliability with lower latency (measured by the number of required LLR calculations at the time when it is output) than RBS, whereas the performance of RBS remains the same as that of the conventional decoding approaches.

REFERENCES

[1] "Study on new radio access technology physical layer aspects," 3GPP, Sophia Antipolis, France, Rep. TR 38.802, Version 14.2.0, 2017.
[2] H. Zhang, N. Liu, X. Chu, K. Long, A.-H. Aghvami, and V. C. M. Leung, "Network slicing based 5G and future mobile networks: Mobility, resource management, and challenges," *IEEE Commun. Mag.*, vol. 55, no. 8, pp. 138–145, Aug. 2017.
[3] H. Nikbakht, M. Wigger, M. Egan, S. Shamai (Shitz), J.-M. Gorce, and H. V. Poor, "An information-theoretic view of mixed-delay traffic in 5G and 6G," *Entropy*, vol. 24, no. 5, p. 637, 2022.
[4] X. Xi, X. Cao, P. Yang, J. Chen, T. Q. S. Quek, and D. Wu, "Network resource allocation for eMBB payload and URLLC control information communication multiplexing in a multi-UAV relay network," *IEEE Trans. Commun.*, vol. 69, no. 3, pp. 1802–1817, Mar. 2021.
[5] B. S. Khan, S. Jangsher, A. Ahmed, and A. Al-Dwei, "URLLC and eMBB in 5G industrial IoT: A survey," *IEEE Open J. Commun. Soc.*, vol. 3, pp. 1134–1163, 2022.
[6] H. Ji, S. Park, J. Yeo, Y. Kim, J. Lee, and B. Shim, "Ultra-reliable and low-latency communications in 5G downlink: Physical layer aspects," *IEEE Wireless Commun.*, vol. 25, no. 3, pp. 124–130, Jun. 2018.
[7] G. Interdonato, S. Buzzi, C. D'Andrea, L. Venturino, C. D'Elia, and P. Vendittelli, "On the coexistence of eMBB and URLLC in multi-cell massive MIMO," *IEEE Open J. Commun. Soc.*, vol. 4, pp. 1040–1059, 2023.
[8] E. Arıkan, "Channel polarization: A method for constructing capacity-achieving codes for symmetric binary-input memoryless channels," *IEEE Trans. Inf. Theory*, vol. 55, no. 7, pp. 3051–3073, Jul. 2009.
[9] I. Tal and A. Vardy, "List decoding of polar codes," *IEEE Trans. Inf. Theory*, vol. 61, no. 5, pp. 2213–2226, May 2015.
[10] A. Alamdar-Yazdi and F. R. Kschischang, "A simplified successive-cancellation decoder for polar codes," *IEEE Commun. Lett.*, vol. 15, no. 12, pp. 1378–1380, Dec. 2011.
[11] B. Li, H. Chen, and D. Tse, "An adaptive successive cancellation list decoder for polar codes with cyclic redundancy check," *IEEE Commun. Lett.*, vol. 16, no. 12, pp. 2044–2047, Dec. 2012.
[12] C. Leroux, A. J. Raymond, G. Sarkis, and W. J. Gross, "A semi-parallel successive-cancellation decoder for polar codes," *IEEE Trans. Signal Process.*, vol. 61, no. 2, pp. 289–299, Jan. 2013.
[13] G. Sarkis, P. Giard, A. Vardy, C. Thibeault, and W. J. Gross, "Fast list decoders for polar codes," *IEEE J. Sel. Areas Commun.*, vol. 34, no. 2, pp. 318–328, Feb. 2016.
[14] S. A. Hashemi, M. Mondelli, S. H. Hassani, C. Condo, R. L. Urbanke, and W. J. Gross, "Decoder partitioning: Towards practical list decoding of polar codes," *IEEE Trans. Commun.*, vol. 66, no. 9, pp. 3749–3759, Sep. 2018.
[15] H. Zhou, C. Zhang, W. Song, S. Xu, and X. You, "Segmented CRC-aided SC list polar decoding," in *Proc. IEEE 83rd Veh. Technol. Conf. (VTC)*, 2016, pp. 1–5.
[16] J. Guo, Z. Shi, Z. Liu, Z. Zhang, and Q. Liu, "Multi-CRC polar codes and their applications," *IEEE Commun. Lett.*, vol. 20, no. 2, pp. 212–215, Feb. 2016.
[17] J. Chen, Y. Chen, K. Jayasinghe, D. Du, and J. Tan, "Distributing CRC bits to aid polar decoding," in *Proc. IEEE Globecom Workshops (GC Wkshps)*, 2017, pp. 1–6.
[18] D. Hui, M. Breschel, and Y. Blankenship, "Interleaved CRC for polar codes," in *Proc. IEEE 87th Veh. Technol. Conf. (VTC)*, 2018, pp. 1–5.
[19] P. Chaki and N. Kamiya, "A novel design of CRC-concatenated polar codes," in *Proc. IEEE Int. Conf. Commun. (ICC)*, 2019, pp. 1–6.
[20] E. Arıkan, "A performance comparison of polar codes and Reed-Muller codes," *IEEE Commun. Lett.*, vol. 12, no. 6, pp. 447–449, Jun. 2008.

[21] A. Elkelesh, M. Ebada, S. Cammerer, and S. Ten Brink, "Belief propagation list decoding of polar codes," *IEEE Commun. Lett.*, vol. 22, no. 8, pp. 1536–1539, Aug. 2018.
[22] A. C. Arli and O. Gazi, "Noise-aided belief propagation list decoding of polar codes," *IEEE Commun. Lett.*, vol. 23, no. 8, pp. 1285–1288, Aug. 2019.
[23] B. Yuan and K. K. Parhi, "Early stopping criteria for energy-efficient low-latency belief-propagation polar code decoders," *IEEE Trans. Signal Process.*, vol. 62, no. 24, pp. 6496–6506, Dec. 2014.
[24] C. Simsek and K. Turk, "Simplified early stopping criterion for belief-propagation polar code decoders," *IEEE Commun. Lett.*, vol. 20, no. 8, pp. 1515–1518, Aug. 2016.
[25] A. Hasani, L. Lopacinski, and E. Grass, "Early stopping of BP polar decoding based on parity-check sums," in *Proc. IEEE 95th Veh. Technol. Conf. (VTC)*, 2022, pp. 1–5.
[26] C. Chen, X. Zhang, Y. Liu, W. Wang, and Q. Zeng, "An ultra-low complexity early stopping criterion for belief propagation polar code decoder," *IEEE Commun. Lett.*, vol. 26, no. 4, pp. 723–727, Apr. 2022.
[27] D. Kim and I.-C. Park, "A fast successive cancellation list decoder for polar codes with an early stopping criterion," *IEEE Trans. Signal Process.*, vol. 66, no. 18, pp. 4971–4979, Sep. 2018.
[28] D. Yang and K. Yang, "Error-aware SCFlip decoding of polar codes," *IEEE Access*, vol. 8, pp. 163758–163768, 2020.
[29] B. Y. Kong, "Bitwise early termination of multiuser detection for IDMA systems," *IEEE Commun. Lett.*, vol. 25, no. 9, pp. 2998–3002, Sep. 2021.
[30] A. Balatsoukas-Stimming, M. H. B. Parizi, and A. Burg, "LLR-based successive cancellation list decoding of polar codes," *IEEE Trans. Signal Process.*, vol. 63, no. 19, pp. 5165–5179, Oct. 2015.
[31] K. Niu and K. Chen, "CRC-aided decoding of polar codes," *IEEE Commun. Lett.*, vol. 16, no. 10, pp. 1668–1671, Oct. 2012.
[32] T. Murata, "Design and analysis of CRC codes for polar codes with successive cancellation list decoding," Ph.D. dissertation, Grad. Eng., Yokohama Nat. Univ., Yokohama, Japan, 2018.
[33] S. A. Hashemi, C. Condo, and W. J. Gross, "Fast simplified successive-cancellation list decoding of polar codes," in *Proc. IEEE Wirel. Commun. Netw. Conf. Workshops (WCNC Wkshps)*, 2017, pp. 1–6.
[34] M. C. Coskun and H. D. Pfister, "An information-theoretic perspective on successive cancellation list decoding and polar code design," *IEEE Trans. Inf. Theory*, vol. 68, no. 9, pp. 5779–5791, Sep. 2022.
[35] H. Ochiai, K. Ikeya, and P. Mitran, "A new polar code design based on reciprocal channel approximation," *IEEE Trans. Commun.*, vol. 71, no. 2, pp. 631–643, Feb. 2023.
[36] P. Trifonov, "Efficient design and decoding of polar codes," *IEEE Trans. Commun.*, vol. 60, no. 11, pp. 3221–3227, Nov. 2012.
[37] H. Ochiai, P. Mitran, and H. V. Poor, "Capacity-approaching polar codes with long codewords and successive cancellation decoding based on improved Gaussian approximation," *IEEE Trans. Commun.*, vol. 69, no. 1, pp. 31–43, Jan. 2021.
[38] T. Murata and H. Ochiai, "On design of CRC codes for polar codes with successive cancellation list decoding," in *Proc. IEEE Int. Symp. Inf. Theory (ISIT)*, 2017, pp. 1868–1872.
[39] T. Murata and H. Ochiai, "Performance analysis of CRC codes for systematic and nonsystematic polar codes with list decoding," *Wireless Commun. Mobile Comput.*, vol. 2018, May 2018, Art. no. 7286909.
[40] "European standard (telecommunications series) EN 300 751 V1.2.1, 2003, radio broadcasting systems; data radio channel (DARC); system for wireless infotainment forwarding and teledistribution," Eur. Telecommun. Stand. Inst., Sophia Antipolis, France, ETSI document EN 300 751 V1.2.1, Jan. 2003.
[41] *FlexRay Communications System Protocol Specification, Version 3.0.1 Ed., FlexRay Consortium*, FlexRay, Arlington, TX, USA, 2010.